

Sawtooth Crashes at High Beta on JET

B Alper, M F F Nave¹, G T A Huysmans, A C C Sips.

JET Joint Undertaking, Abingdon, Oxon, OX14 3EA.

¹ Associação EURATOM/IST, Instituto Superior Tecnico, Lisbon, Portugal.

"This document is intended for publication in the open literature. It is made available on the understanding that it may not be further circulated and extracts may not be published prior to publication of the original, without the consent of the Publications Officer, JET Joint Undertaking, Abingdon, Oxon, OX14 3EA, UK".

"Enquiries about Copyright and reproduction should be addressed to the Publications Officer, JET Joint Undertaking, Abingdon, Oxon, OX14 3EA".

INTRODUCTION

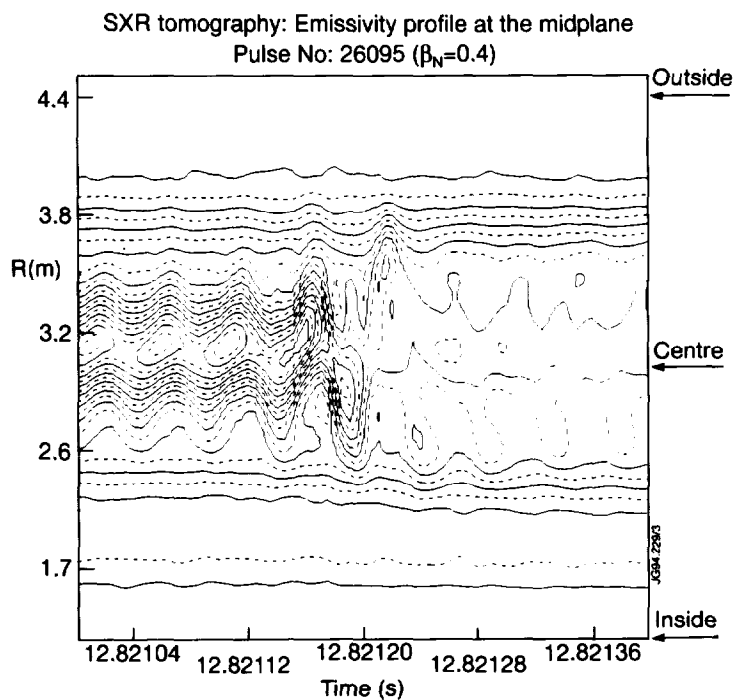
Sawteeth observed in high performance discharges on JET are observed to have features which extended well beyond the $q=1$ surface. Those sawteeth which occur at high beta often couple to a giant ELM typically within $50\mu\text{s}$ and, in all such cases, an irrecoverable fall in fusion yield results [1]. Similar phenomena have been observed in other high beta discharges on JET where an ELM is also observed to couple to the sawtooth collapse. In these discharges, with low values of toroidal magnetic field, a sequence of sawtooth/ELM events occurs which is associated with a saturation in beta [2,3].

COMPARISON OF SAWTOOTH CRASHES AT LOW AND MEDIUM BETA

Features which are clearly identified in sawtooth collapses at low beta such as mixing radii and heat pulses can become somewhat obscured as beta increases. Here we define low beta to correspond to values of $\beta_N < 0.35$ with β_N defined to be the toroidal beta, normalised to the Troyon limit: $\beta_T = 2.8 I(\text{MA})/a(\text{m})B_\phi(\text{T})$. The main cause of this is a fast perturbation associated with the final stages of the $(m,n)=(1,1)$ precursor mode of the sawtooth collapse which is observed to extend well beyond the inversion radius in medium and high beta

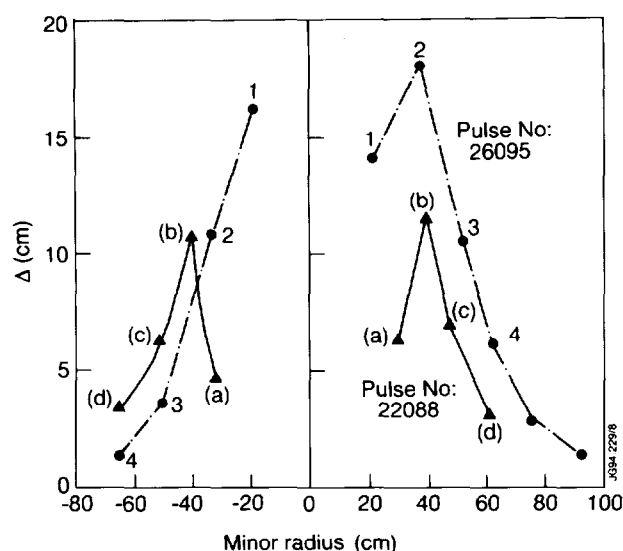
sawteeth. A noticeable ballooning effect is found with pronounced bulging of flux surfaces on the low field side in these cases. This is shown in **Figure 1**, a contour plot of soft X-ray (SXR) intensity vs time for a sawtooth crash at $\beta_N=0.4$.

Figure 1 Contour plot of SXR emissivities for an intermediate-beta sawtooth showing a bulge in the flux surfaces on the low field side, between $R=3.6\text{m}$ and 3.9m , at the time of the collapse.



We determined of the magnitude of the deviation (or excursion) of these flux surfaces from their mean value as a function of radius for discharges with different beta. The results of the **maximum** excursion of a flux surface during the sawtooth is plotted for a low and intermediate beta discharge in **Figure 2**. In the low beta discharge, (22088, $\beta_N=0.2$) the deviation is seen to be reasonably symmetric between the low and high field sides and to fall off rapidly beyond the inversion radius of ~ 40 cms. The intermediate beta discharge, 26095, shows a pronounced ballooning effect, with the field line excursion extending to large values of minor radius on the low field side just stopping short of the plasma edge at $a=120$ cms.

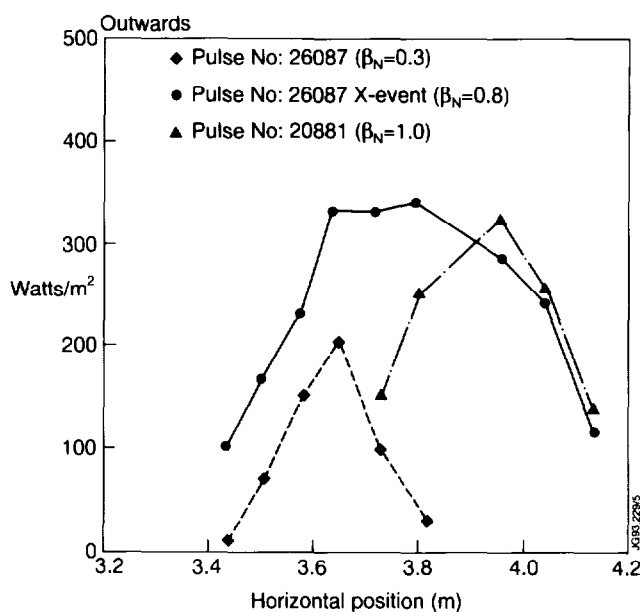
Figure 2. Comparison, between two discharges, of the maximum deviation of flux surfaces with minor radius, during a sawtooth collapse - one at low beta (22088), the other at intermediate beta (26095). Evidence of a ballooning effect on the low field side is apparent in shot 26095.



SAWTOOTH CRASHES AT HIGH BETA

The pronounced bulging of the flux surfaces - the sawtooth excursion as we have called it here - is observed to extend to larger radii as beta increases. This is illustrated in **Figure 3**. The figure shows how the magnitude of the perturbation of the line-integrated SXR signals varies with radius at different beta values. The high beta sawteeth ($\beta_N > 0.5$) clearly show the perturbation in SXR intensity extending right to the plasma edge especially in the outward (low field) direction. The perturbation is transient, lasting usually less than 30 μ s.

Figure 3. An illustration of how the sawtooth perturbation grows with beta. The magnitude of the perturbation in line integrated SXR emission is plotted as a function of radius. The perturbation, at high beta, can be seen to extend to the outside plasma edge.



COUPLING OF THE HIGH BETA SAWTEETH TO AN ELM

In most of the high beta discharges ($\beta_N > 0.5$) an ELM appears soon after the sawtooth crash i.e. within 25-60 μ s. This, we believe, is a direct consequence of the sawtooth perturbation extending to the edge on the low field side as discussed above. In the case of the hot-ion H-mode discharges, a giant ELM appears about 50 μ s after the sawtooth, initially localised close to the plasma X-point and is followed within a few milliseconds by an influx of carbon impurities which cool the plasma. This event can occur either at peak neutron yield or up to 300ms afterwards but in all cases the plasma fails to recover its high performance.

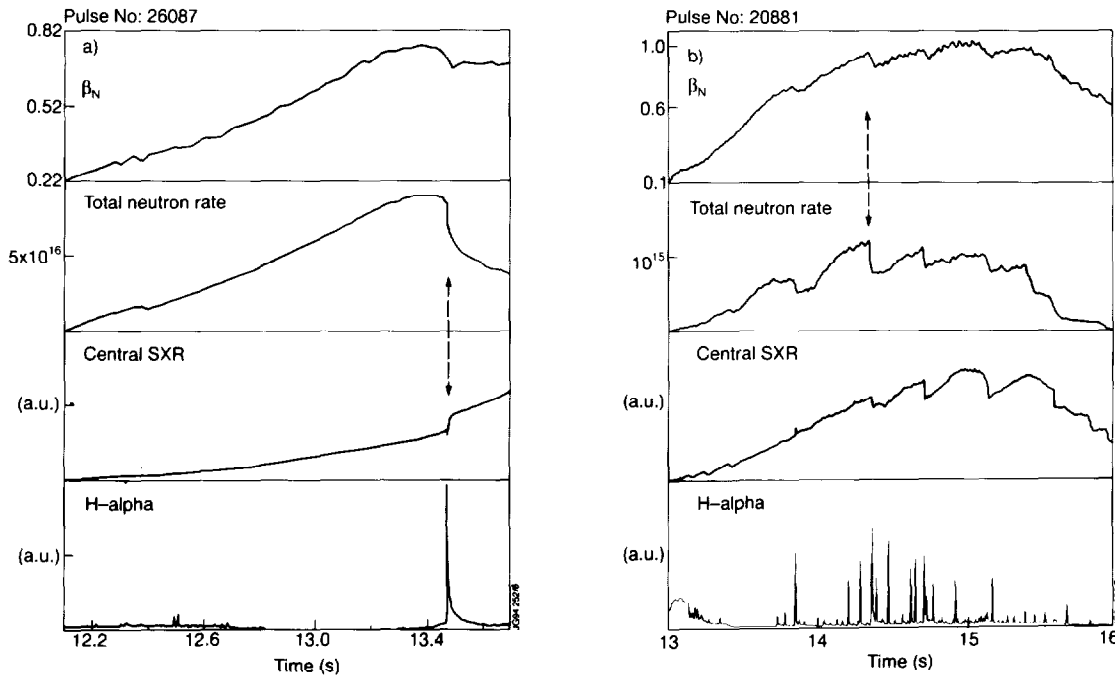


Figure 4. Traces of β_N , neutron yield, central soft X-rays and H-alpha for (a) the hot-ion H-mode discharge 26087 and (b) the low field high-beta discharge 20881. The dotted lines indicate the sawtooth events shown in figure 3 for these discharges.

In the high beta, low toroidal field, discharges, with lower power input to the plasma, an ELM occurs within 30 μ s of the sawtooth crash. Although the plasma can recover to similar values of beta afterwards, the process repeats itself and leads to a limitation in beta. Other ELMs and fishbone activity are present during this period which may also contribute to saturation in beta [4]. Figure 4 illustrates these effects.

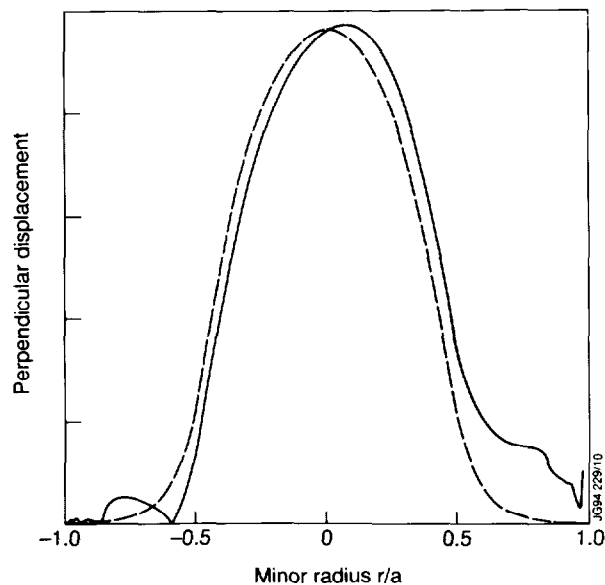
MODELLING

To compare the experimental results with theoretical mode structures, the eigenfunction of the internal kink mode has been calculated for different values of β , using the CASTOR toroidal stability code [5]. At low beta the displacement of the internal kink mode has a predominantly $m=1$ structure which does not extend far beyond the $q=1$ surface. The higher harmonics, which are due to toroidicity are relatively small. In contrast, Figure 5 shows the computed mode structure of the internal kink of a high performance discharge at high β

(#26087, $\beta_N=0.8$). The amplitude falls off only slowly beyond the $q=1$ surface and is finite at the plasma boundary due to the coupling to the higher poloidal harmonics ($m \geq 2$). There is also a marked difference between the low and high field side. The poloidal harmonics generally add on the low field side whereas they tend to cancel each other on the high field side - a (low- n) manifestation of ballooning.

The amplitude of all the $m \geq 2$ harmonics relative to the $m=1$ harmonic increases linearly with β_p [6]. In the hot-ion H-mode discharges, this magnetic coupling is enhanced by the large radius of the $q=1$ surface [1]. Further, a finite edge current density can increase the mode amplitude locally at the plasma boundary.

Figure 5. The displacement perpendicular to the flux surfaces as a function of the minor radius for the high performance discharge 26087. The full line is the absolute value of total displacement along the horizontal axis, the dotted line is the $m=1$ harmonic.



CONCLUSIONS

The sawtooth crashes on JET display features which depend on β . The main observation is a transient bulging of flux surfaces (duration $<30\mu\text{s}$), which is predominantly on the low field side and extends to larger radii as β increases. This phenomenon reaches the plasma boundary when β_N exceeds 0.5 and in these cases is followed by an ELM within $50\mu\text{s}$. These sawtooth/ELM events limit plasma performance. Modelling of mode coupling shows qualitative agreement between observations of the structure of the sawtooth precursor and the calculated internal kink mode at high β .

REFERENCES

- [1] M.F.F. Nave et al, MHD activity in JET hot ion H-mode discharges, submitted to Nuclear Fusion
- [2] The Jet Team, Proc. of 13th IAEA Conf. on Plasma Physics and Contr. Fus. Research, Washington, Vol.1(1990) 219
- [3] P. Smeulders et al, this conference
- [4] M.F.F. Nave et al., Nucl. Fus. 31(1991) 697
- [5] W. Kerner et al., Proc. 18th EPS Berlin (1991), part IV, p.89-93.
- [6] M.F.F. Nave et al., Proc. 20th EPS Lisbon (1993).